The Monogenic Signal

Michael Felsberg and Gerald Sommer

***Abstract*—This paper introduces a two-dimensional (2-D) generalization of the analytic signal. This novel approach is based on the Riesz transform, which is used instead of the Hilbert transform. The combination of a 2-D signal with the Riesz transformed one yields a sophisticated 2-D analytic signal: the monogenic signal. The approach is derived analytically from irrotational and solenoidal vector fields. Based on local amplitude and local phase, an appropriate local signal representation that preserves the split of identity, i.e., the invariance-equivariance property of signal decomposition, is presented. This is one of the central properties of the one–dimensional (1-D) analytic signal that decomposes a signal into structural and energetic information. We show that further properties of the analytic signal concerning symmetry, energy, allpass transfer function, and orthogonality are also preserved, and we compare this with the behavior of other approaches for a 2-D analytic signal. As a central topic of this paper, a geometric phase interpretation that is based on the relation between the 1-D analytic signal and the 2-D monogenic signal established by the Radon transform is introduced. Possible applications of this relationship are sketched, and references to other applications of the monogenic signal are given.**

***Index Terms*—Analytic signal, Hilbert transform, Radon transform, Riesz transform.**

I. Introduction

THE analytic signal is an important complex-valued representation in one-dimensional (1-D) signal processing, which is used in various applications like coding information (phase and frequency modulation), radar-based object detection, processing of seismic data [1], speech recognition, airfoil design [2], etc. Some of these applications can be related to problems in image processing, which is based on 2-D signal processing. For example, the demodulation of 2-D functions is the problem we encounter if we want to recover the shape of a surface from an interferogram [3]. Furthermore, the local frequency can be taken as a measure for local scale (i.e., the frequency band) [4]; structures such as lines and edges can be distinguished by the local phase [5]; the local amplitude and the local phase can be used for edge detection [6], and the local phase can be used to estimate the disparity of stereo images [7] or the flow in image sequences.

From the viewpoint of image processing and recognition, the fundamental property of the analytic signal is the *split of identity*. This means that in its polar representation, the modulus of the complex signal is identified as a local quantitative measure of a signal called the *local amplitude*, and the argument of the complex signal is identified as a local measure for the qualitative information of a signal called the *local phase*. Local amplitude and local phase fulfill the properties of *invariance* and *equivariance* [5]. This means that the local phase is invariant with respect to the local energy of the signal but changes if the local structure varies. The local amplitude is invariant with respect to the local structure but represents the local energy. Energy and structure are independent information contained in a signal unless the signal is a combination of partial signals with different local phases on different scales. In the latter case, to maintain the invariance-equivariance property, the signal must be bandpass filtered in order to remove the other partial signals. Quadrature (mirror) filters are well-known operators [5] that deliver bandpass filtered amplitude and phase information. Since it is (at least approximately) possible to separate the signal into its partial signals by using narrow bandpass filters, we can think of the *polar representation* of the analytic signal in a narrow frequency band as an *orthogonal decomposition* of information. We will use the terms *structural information* and *energetic information* in the following. This terminology also gives hints for designing methods for automatic image understanding since the main information is carried by the phase [8].

The analytic signal for the 1-D case is well known, and from the discussion above, we can say that a sophisticated generalization of the analytic signal to two dimensions should keep the idea of the orthogonal decomposition of the information. Hence, it should have a representation that is invariant and equivariant with respect to energetic and structural information. The problem now is that a 1-D measure like the local phase cannot encode 2-D structure because it does not have enough degrees of freedom. Indeed, the commonly used generalization obtained by calculating the Hilbert transform with respect to one of the axes of the image coordinate system (or an arbitrary preference direction [5]) is not isotropic. Therefore, local phase and local amplitude are affected by a systematic error that depends on the angle between the axes (or the preference direction) and the orientation of the signal. This problem is equivalent to the design of an isotropic odd 2-D filter (which is not possible in the complex domain [6]) or to the solution of the 2-D dispersion equation (which is also not possible, according to [9] and [10]). In our opinion, the reason for the failure thus far in designing an appropriate 2-D analytic signal is the restriction to the algebra of complex numbers. In his thesis [11], Bülow chose hypercomplex algebras in order to design a local phase concept of 2-D signals. Nevertheless, the local energy of his quaternionic analytic signal is, in general, not constant if the orientation of the signal is changed, i.e., it is not isotropic. Hence, the invariance-equivariance property is not perfectly fulfilled with respect to rotations. More details about these approaches for a 2-D analytic signal will be given in the beginning of Section III.

Manuscript received September 15, 2000; revised September 11, 2001. This work was supported by the German National Merit Foundation by DFG Grants Graduiertenkolleg 357 (M. Felsberg) and So-320-2-2 (G. Sommer).

The authors are with the Cognitive Systems Group, Christian Albrechts University of Kiel, Kiel, Germany (e-mail: mfe@ks.informatik.uni-kiel.de).

Publisher Item Identifier S 1053-587X(01)10479-4.

In this paper, we also make use of the quaternions. However, in contrast to Bülow, we retain a 1-D phase but add the *orientation information* to the quaternionic representation of the signal. This yields an approach that takes the locally strongest *intrinsically 1-D* [12] structure and encodes it in the classical 1-D phase. Its orientation is encoded in a new component that we call, according to local phase and local amplitude, the *local orientation*. Since orientation is a geometric property, we call this information *geometric information*. For intrinsically 2-D signals, the properties of our new generalization, which we call the *monogenic signal*, will be discussed in the context of the relationship between the 1-D phase and the monogenic phase established by the Radon transform. The monogenic signal is also related to the structure tensor (e.g., [5]), but in contrast to that, it is *linear*. Actually, we derived it starting from the structure tensor. Our result can be considered as a combination of the analytic signal with the orientation vector obtained from the structure tensor. Therefore, in the first published result [13], we used the term "structure multivector," which is now used for an extended approach [14].

II. Preliminaries

In this section, we give the mathematical framework for what follows. Originally, we derived the monogenic signal using geometric algebra (see e.g., [15] and [16]) and Clifford analysis (e.g., [17]). The formulation in geometric algebra is preferable because some notational problems are avoided, and the derivation is straightforward (see [18]). Nevertheless, since geometric algebra is less widely known, we formulate our approach in vector notation. The only exceptions are some formulae where we make use of the algebra of quaternions.

Throughout this paper, we use the following notation.

- The considered (real) *signals* (or images) are 1-D or 2-D functions f, which are continuously differentiable and in L^2 so that all mentioned transforms can be performed.
- While scalars and quaternions are denoted by italic letters, *vectors* in $\mathbb{R}^n$ are represented by boldface letters $\mathbf{x} = (x_1, x_2, \ldots, x_n)^\top$ ($\top$ indicates the transpose). The scalar product is denoted by $\langle \cdot, \cdot \rangle$. In 2-D, one vector orthogonal to $\mathbf{x} = (x_1, x_2)^\top$ is $\mathbf{x}^\perp = (x_2, -x_1)^\top$. In 3-D, $\mathbf{x} \times \mathbf{y}$ indicates the cross product.
- The n-D *Fourier transform* $(n = 1, 2)$ of $f(\mathbf{x})$ is denoted by

$$F(\mathbf{u}) = \mathcal{F}_n\{f(\mathbf{x})\} = \int_{\mathbb{R}^n} f(\mathbf{x}) \exp(-i2\pi\langle \mathbf{x}, \mathbf{u} \rangle)\, d\mathbf{x}.$$

- The algebra of *quaternions* $\mathbb{H}$ is spanned by $\{1, i, j, k\}$, and the product is defined by $i^2 = j^2 = -1$ and $ij = -ji = k$. Further details about quaternions are summarized in the Appendix. We sometimes switch between 2-D vectors and quaternions by $(i, j)\mathbf{x} = x_1 i + x_2 j$ and between 3-D vectors and quaternions by $(i, j, 1)\mathbf{x} = x_3 + x_1 i + x_2 j$. The conjugate of a quaternion q is denoted by $\bar{q}$ and its norm by $|q|$.
- The *Hilbert transform* is defined by the transfer function

$$H_1(u) = i \operatorname{sign}(u)$$

and the transformed signal is denoted $f_H(x)$ [4]. The *analytic signal* is given by $f_A(x) = f(x) - i f_H(x)$.

III. Hilbert Transform

As a motivation for the following sections, we recall some properties of the Hilbert transform and the analytic signal in 1-D. We show that some of these properties are lost for the known 2-D approaches. Furthermore, we present a derivation of the Hilbert transform from 2-D vector fields that will be generalized to 2-D in Section IV-A.

A. Hilbert Transform and Analytic Signal in 1-D and 2-D

The Hilbert transform has some important properties that should be preserved in its 2-D generalization.

- It is anti-symmetric: $H_1(-u) = -H_1(u)$.
- It suppresses the DC component: $H_1(0) = 0$.
- Its energy is equal to one for all nonzero frequencies: $|H_1(u)| = 1\ \forall u \neq 0$.

Accordingly, the analytic signal has the following properties.

- Its energy is two times the energy of the original signal (if the DC component is neglected) because f and f_H are orthogonal.
- The analytic signal performs a split of identity (see Section I).
- The spectrum of an analytic signal is one sided:

$$H_1(u) = 0 \quad \forall u < 0.$$

Since the 2-D Hilbert transform is a key to designing a 2-D analytic signal, we concentrate on approaches involving it. As far as we know, the following approaches for generalizing the Hilbert transform to higher dimensions can be found in the literature (for a more extensive discussion, see [11]).

- *Partial Hilbert transform:* The Hilbert transform is performed with respect to a half-space that is chosen by introducing a *preference direction* [5]:

$$H_P(\mathbf{u}) = i \operatorname{sign}(\langle \mathbf{u}, \mathbf{n} \rangle).$$

  The Hilbert transform performed with respect to one of the axes is a special case of the partial Hilbert transform. The main drawback is the missing isotropy of the transform.
- *Total Hilbert transform;* The Hilbert transform is performed with respect to both axes:

$$H_T(\mathbf{u}) = -\operatorname{sign}(u_1)\operatorname{sign}(u_2)$$

  (see [19]). This approach is not a valid generalization of the Hilbert transform since it does not perform a phase shift of $\pi/2$.
- A combination of partial Hilbert transforms and the total Hilbert transform in the complex Fourier domain yields a one-quadrant analytic signal [19]:

$$H_Q(\mathbf{u}) = i(\operatorname{sign}(u_1) + \operatorname{sign}(u_2) + \operatorname{sign}(u_1)\operatorname{sign}(u_2)).$$

  This approach is neither complete nor isotropic.
- *Combined partial and total Hilbert transforms in the quaternionic Fourier domain:* Instead of using the com-

plex Fourier transform, the quaternionic Fourier transform [20] is used. The result is discussed in detail in [11]. As already pointed out in the introduction, this approach is not isotropic either.

Hence, a common drawback of all previous approaches is the missing isotropy that is necessary to obtain the invariance-equivariance property. Other properties of the 1-D Hilbert transform can easily be checked by calculation and are discussed in detail in [11].

B. Derivation of the Hilbert Transform

The Hilbert transform of 1-D signals emerges from complex analysis by means of the Cauchy formula [19]. Therefore, it is straightforward to derive an appropriate 2-D generalization of the Hilbert transform by means of the higher dimensional generalization of complex analysis known as Clifford analysis [17]. In the same manner as geometric algebra, Clifford analysis is less widely known; therefore, we choose vector field theory to perform the derivations. It is a well-known fact that *analytic functions*[1] correspond directly to 2-D harmonic fields [21]. This generalizes to 3-D such that *monogenic functions*[2] correspond to 3-D harmonic fields. This equivalence is used in Section IV-A to derive the Riesz transform as a 2-D generalization of the Hilbert transform. The aim of this section is to derive the Hilbert transform by means of 2-D harmonic fields. We show that the Hilbert transform relates the components of such a vector field on every line with arbitrary but fixed x_2.

A harmonic potential p is a solution of the Laplace equation

$$\Delta p = \langle \nabla, \nabla \rangle p = 0$$

where $\nabla = ((\partial/\partial x_1), (\partial/\partial x_2))^\top$. The gradient field of p yields the harmonic potential field

$$\mathbf{g}(\mathbf{x}) = (g_1(\mathbf{x}), g_2(\mathbf{x}))^\top = \nabla p(\mathbf{x}).$$

In this derivation, we restrict the Laplace equation to the open domain $x_2 < 0$, with the boundary condition $g_2(x_1, 0) = f(x_1)$ (boundary value problem of the second kind) yielding the solution p, depending on f. The same solution can be obtained by an appropriate choice for the boundary condition $g_1(x_1, 0)$, and we show that this boundary condition is given by the Hilbert transform of f : $f_H(x_1) = g_1(x_1, 0)$ (see also Fig. 1).

The harmonic potential field $\mathbf{g}$ is irrotational and solenoidal in the half space $x_2 < 0$

$$\operatorname{rot} \mathbf{g}(\mathbf{x}) = \langle \nabla, \mathbf{g}(\mathbf{x})^\perp \rangle = \frac{\partial g_2(\mathbf{x})}{\partial x_1} - \frac{\partial g_1(\mathbf{x})}{\partial x_2} = 0 \quad \text{and} \tag{1}$$

$$\operatorname{div} \mathbf{g}(\mathbf{x}) = \langle \nabla, \mathbf{g}(\mathbf{x}) \rangle = \frac{\partial g_1(\mathbf{x})}{\partial x_1} + \frac{\partial g_2(\mathbf{x})}{\partial x_2} = 0 \tag{2}$$

[1]In mathematics, these functions are also called *holomorphic*. Such functions are characterized by having a local power series expansion about each point [21].

[2]Originally, monogenic was another, somewhat archaic term for holomorphic [21]. In Clifford analysis literature, it was reused to express the multidimensional character of the functions.

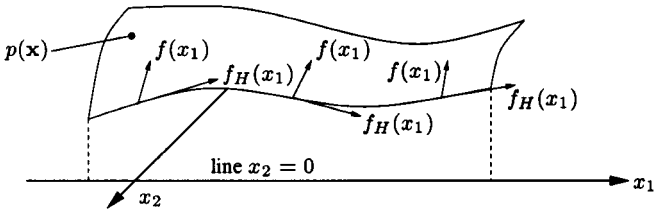

Fig. 1. Harmonic potential $p(\mathbf{x})$ for $x_2 < 0$ and its gradient field on the boundary $x_2 = 0$, which is given by the 1-D function $f(x_1)$ and its Hilbert transform $f_H(x_1)$.

where (1) follows from $\mathbf{g}$ being a gradient field, and (2) follows from p being harmonic. If we identify $\mathbb{R}^2$ with the complex plane according to

$$z = (i, 1)\mathbf{x} = x_2 + ix_1$$

and embed $\mathbf{g}$ as

$$g_{\mathbb{C}} = (-i, 1)\mathbf{g} = g_2 - ig_1$$

these equations are the Cauchy–Riemann equations, which are solved by analytic functions.

There are several ways to solve (1) and (2). One is to take the partial derivatives of the *fundamental solution* of the 2-D Laplace equation ($p(\mathbf{x}) = \log|\mathbf{x}|$). Since we are only interested in the relationship between g_1 and g_2, it is easier to perform the calculations in the frequency domain of x_1, which means that we apply the 1-D Fourier transform $\mathcal{F}_1$. From (2), it follows that

$$\begin{aligned}\mathcal{F}_1\{\operatorname{div}\mathbf{g}(\mathbf{x})\}(u_1) &= i2\pi u_1 G_1(u_1, x_2) + \frac{\partial}{\partial x_2} G_2(u_1, x_2) \\ &= 0\end{aligned}$$

and by plugging in $\mathbf{g} = \nabla p$ (i.e., using (1))

$$-4\pi^2 u_1^2 P(u_1, x_2) + \frac{\partial^2}{\partial x_2^2} P(u_1, x_2) = 0.$$

This differential equation is solved for $x_2 < 0$ by

$$P(u_1, x_2) = C(u_1) \exp(2\pi |u_1| x_2)$$

where $C(u_1)$ is independent of x_2. Therefore, the components of the gradient field are

$$\begin{aligned} G_1(u_1, x_2) &= i2\pi u_1 P(u_1, x_2) \quad \text{and} \\ G_2(u_1, x_2) &= 2\pi |u_1| P(u_1, x_2). \end{aligned}$$

Since $\mathbf{g}$ can be considered to be an analytic function $g_{\mathbb{C}}$, the component g_1 is the harmonic conjugate of g_2 and vice versa [21], which is another way to say that g_1 and g_2 are a Hilbert pair

$$G_1(u_1, x_2) = i \operatorname{sign}(u_1) G_2(u_1, x_2) = H_1(u_1) G_2(u_1, x_2).$$

Hence, for any fixed $x_2 < 0$, the Hilbert transform relates the components of a harmonic potential field. This relationship also holds for the continuous extension of $\mathbf{g}$ for $x_2 \to -0$

$$G_1(u_1, 0) = H_1(u_1) G_2(u_1, 0) = H_1(u_1) F(u_1).$$

Applying the inverse Fourier transform to this expression yields $f_H(x_1) = g_1(x_1, 0)$, and therefore, $f_A(x_1) = g_{\mathbb{C}}(x_1, 0)$ is consistent with the definition of the analytic signal. Hence, we have established a fundamental relationship between 2-D harmonic potential fields and the 1-D analytic signal.

IV. New 2-D Analytic Signal

Our new 2-D analytic signal is based on a 2-D generalization of the Hilbert transform known as the Riesz transform [22][3] that is derived in the next section. The combination of the signal and the Riesz-transformed one forms our new 2-D analytic signal (the monogenic signal), which is defined in Section IV-B using an embedding in the algebra of quaternions.

A. Riesz Transform

In the light of the previous section, we start with a 3-D harmonic potential p for deriving the Riesz transform. The boundary condition of the 3-D Laplace equation is a 2-D function, and hence, the choice of dimension is appropriate for 2-D signals. As we show in Section V-A, the additional degree of freedom allows us to encode the local orientation of the signal.

According to the derivation of the Hilbert transform, we show that the three boundary conditions of the 3-D Laplace equation are related by the Riesz transform (see also [23]), and hence, the Riesz transform replaces the Hilbert transform when proceeding from 2-D to 3–D. Denoting the harmonic potential field as

$$\mathbf{g}(\mathbf{x}) = (g_1(\mathbf{x}), g_2(\mathbf{x}), g_3(\mathbf{x}))^\top = \nabla p(\mathbf{x})$$

(where ∇ is the 3-D gradient operator), the boundary condition reads $g_3(x_1, x_2, 0) = f(x_1, x_2)$. The relation of $g_3(x_1, x_2, 0)$ to the other two boundary conditions $g_1(x_1, x_2, 0)$ and $g_2(x_1, x_2, 0)$ yields the definition of the Riesz transform.

The harmonic potential field $\mathbf{g}$ is irrotational and solenoidal in the half-space $x_3 < 0$

$$\operatorname{rot} \mathbf{g}(\mathbf{x}) = \nabla \times \mathbf{g}(\mathbf{x}) = 0 \quad \text{and} \tag{3}$$

$$\operatorname{div} \mathbf{g}(\mathbf{x}) = \langle \nabla, \mathbf{g}(\mathbf{x}) \rangle = 0 \tag{4}$$

where (3) follows from $\mathbf{g}$ being a gradient field, and (4) follows from p being harmonic. As before, we do not solve the equations using the fundamental solution of the 3–D Laplace equation ($p(\mathbf{x}) = |\mathbf{x}|^{-1}$), but instead perform the calculations in the frequency domain of x_1 and x_2. This means that we apply the 2-D Fourier transform $\mathcal{F}_2$. Accordingly, we get from (4) the differential equation

$$\frac{\partial^2}{\partial x_3^2} P(u_1, u_2, x_3) = 4\pi^2 q^2 P(u_1, u_2, x_3)$$

with $q = \sqrt{u_1^2 + u_2^2}$. Solving this equation for $x_3 < 0$ yields

$$P(u_1, u_2, x_3) = C(u_1, u_2) \exp(2\pi q x_3)$$

where $C(u_1, u_2)$ is independent of x_3. Consequently, we obtain for $\mathbf{g} = \nabla p$ (i.e., applying (3))

$$G_1(u_1, u_2, x_3) = i2\pi u_1 P(u_1, u_2, x_3) \tag{5}$$

$$G_2(u_1, u_2, x_3) = i2\pi u_2 P(u_1, u_2, x_3) \tag{6}$$

$$G_3(u_1, u_2, x_3) = 2\pi q P(u_1, u_2, x_3). \tag{7}$$

Finally, we get the relations between G_1, G_2, and G_3

$$G_1(u_1, u_2, x_3) = \frac{iu_1}{q} G_3(u_1, u_2, x_3) \tag{8}$$

$$G_2(u_1, u_2, x_3) = \frac{iu_2}{q} G_3(u_1, u_2, x_3). \tag{9}$$

Hence, for any fixed $x_3 < 0$, the components of a harmonic potential field are related by (8) and (9). This relationship also holds for the continuous extension of $\mathbf{g}$ for $x_3 \to -0$

$$G_1(u_1, u_2, 0) = \frac{iu_1}{q} G_3(u_1, u_2, 0) = \frac{iu_1}{q} F(u_1, u_2) \quad \text{and}$$

$$G_2(u_1, u_2, 0) = \frac{iu_2}{q} F(u_1, u_2).$$

Setting

$$\mathbf{F}_R(u_1, u_2) = (G_1(u_1, u_2, 0), G_2(u_1, u_2, 0))^\top$$

and defining $\mathbf{u} = (u_1, u_2)^\top$ so that $q = |\mathbf{u}|$, we get the expression of the Riesz-transformed signal in the frequency domain

$$\mathbf{F}_R(\mathbf{u}) = \frac{i\mathbf{u}}{|\mathbf{u}|} F(\mathbf{u}) \stackrel{\text{def}}{=} \mathbf{H}_2(\mathbf{u}) F(\mathbf{u}). \tag{10}$$

The transfer function of the Riesz transform[4] $\mathbf{H}_2$ constitutes a 2-D generalization of the Hilbert transform. In the following, we use the notation $\mathbf{x} = (x_1, x_2)^\top$ since $x_3 = 0$. The multiplication in the Fourier domain in (10) corresponds to the following convolution in the spatial domain:

$$\mathbf{f}_R(\mathbf{x}) = -\frac{\mathbf{x}}{2\pi |\mathbf{x}|^3} * f(\mathbf{x}) \stackrel{\text{def}}{=} \mathbf{h}_2(\mathbf{x}) * f(\mathbf{x}) \tag{11}$$

where $\mathbf{h}_2$ is obtained by applying the derivative theorem of the Fourier transform to $\mathcal{F}_2\{|\mathbf{x}|^{-1}\} = |\mathbf{u}|^{-1}$ [24] (see also [22]). Hence, we have established the Riesz transform to be an appropriate 2-D generalization of the Hilbert transform in the context of a vector field-based derivation.

B. Monogenic Signal

In Section III, we used the analogy between 2-D vector fields and complex functions to obtain the complex-valued analytic signal $f_A(x_1) = g_{\mathbb{C}}(x_1, 0)$. The algebra of complex numbers is not sufficient to embed a generalized 2-D analytic signal, consisting of the signal f and its Riesz transform vector $\mathbf{f}_R$, since we have three components now. Actually, function theory corresponding to 3-D (and nD) vector fields is given by means of Clifford analysis [17]. If we embed $\mathbb{R}^3$ into the subspace of $\mathbb{H}$ spanned by $\{1, i, j\}$ according to

$$q = (i, j, 1)\mathbf{x} = x_3 + x_1 i + x_2 j$$

[3]Here, we want to thank T. Bülow for alluding to the existence of the Riesz transform and for giving us [22] and [23], which enabled us to identify the transform (8) in [13] as such.

[4]Our definition of the Riesz transform differs to those in [22] by a minus sign due to $x_3 < 0$ instead of $x_3 > 0$.

and embed the vector field $\mathbf{g}$ as

$$g_{\mathbb{H}} = (-i, -j, 1)\mathbf{g} = g_3 - g_1 i - g_2 j,$$

then (4) and (3) are equivalent to the generalized Cauchy–Riemann equations from Clifford analysis [17]. Functions that fulfill these equations are called (left) *monogenic* functions. Accordingly, we define the *monogenic signal* using the same embedding by the transfer function

$$\begin{aligned} F_M(\mathbf{u}) &= G_3(u_1, u_2, 0) - iG_1(u_1, u_2, 0) - jG_2(u_1, u_2, 0) \\ &= F(\mathbf{u}) - (i, j)\mathbf{F}_R(\mathbf{u}) = \frac{|\mathbf{u}| + (1, k)\mathbf{u}}{|\mathbf{u}|} F(\mathbf{u}) \end{aligned} \quad (12)$$

which is equivalent to

$$f_M(\mathbf{x}) = f(\mathbf{x}) - (i, j)\mathbf{f}_R(\mathbf{x}). \quad (13)$$

Note that we have moved the imaginary units i and j to the left to obtain a compact expression ($\mathbb{H}$ is a skew field, i.e., noncommutative).

Now, having defined the monogenic signal as a 2-D generalization of the analytic signal, we check whether the properties of the latter are fulfilled. First, we look at some properties of the Riesz transform.

- It is antisymmetric since $\mathbf{H}_2(-\mathbf{u}) = -\mathbf{H}_2(\mathbf{u})$. Note in this context that symmetry in 2-D can be with respect to a point or to a line. The choice of symmetry is fundamental to designing the generalization of the Hilbert transform (in 1-D, there is only one symmetry). Obviously, the Riesz transform corresponds to point symmetry, whereas the approach in [11] corresponds to line symmetry with respect to the coordinate axes, and the partial Hilbert transform corresponds to line symmetry with respect to the preference direction.
- It suppresses the DC component. We have a singularity at $\mathbf{u} = 0$. If we remove it by continuously extending the two components of the Riesz transform along the lines $u_1 = 0$ [see (8)] and $u_2 = 0$ [see (9)], we immediately get $\mathbf{H}_2(0) = 0$.
- The energy has value one for all nonzero frequencies: $|\mathbf{H}_2(\mathbf{u})| = 1\ \forall \mathbf{u} \neq 0$. This follows directly from the definition of $\mathbf{H}_2(\mathbf{u})$ in (10).

These properties can be verified by considering the vector field $\mathbf{H}_2$ (see Fig. 2).

According to the properties of the Riesz transform, and in comparison with the analytic signal, the monogenic signal has the following properties:

- Its energy is two times the energy of the original signal if the DC component is neglected:

$$\int |f_M(\mathbf{x})|^2 \, d\mathbf{x} = \int f(\mathbf{x})^2 + |\mathbf{f}_R(\mathbf{x})|^2 \, d\mathbf{x} = 2 \int f(\mathbf{x})^2 \, d\mathbf{x}.$$

- In polar coordinates, the monogenic signal fulfills the split of identity. Since the energy is only modified by a constant real factor, we conclude that the amplitude of the monogenic signal is *isotropic*, which means that there is no dependence on the orientation of a signal (see also Fig. 3). This can be compared with the isotropy property of the structure tensor, which fulfills the invariance-equivariance property with respect to energy and orientation (but not phase). Further details will be discussed in Section V-B.
- The spectrum of the monogenic signal is not one-sided, i.e., it includes redundancies, but this property is irrelevant for image recognition. Nevertheless, it is possible to use a nonredundant representation [13].

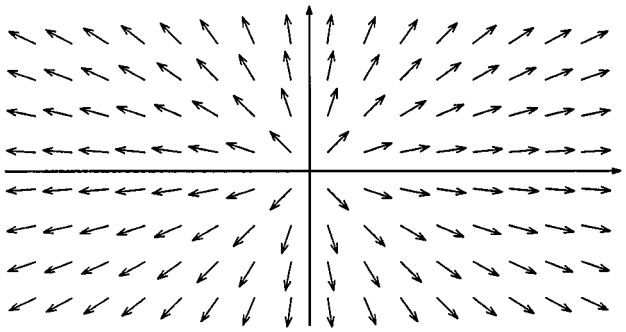

Fig. 2. Transfer function of the Riesz transform displayed as a vector field. The axes are the frequencies u_1 and u_2. The vector field is given by the normalized frequency vectors [see (10)] and by setting it to zero at the origin (see text).

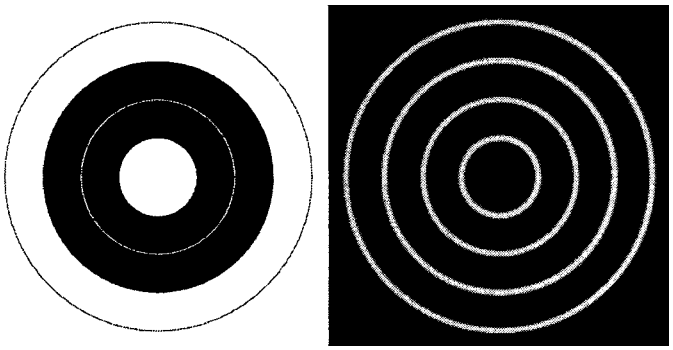

Fig. 3. Left: Test image showing all even and odd symmetries for all orientations. Right: Energy of the corresponding monogenic signal is isotropic and independent of the local symmetry.

V. Interpretation of the Monogenic Signal

In order to obtain an appropriate 2-D analytic signal, we introduce a phase approach for the monogenic signal in the next section. The relation of the new phase to the 1-D phase is then discussed in Section V-B.

A. Phase of the Monogenic Signal

The phase of a complex signal is a measure of the rotation of a real signal in the complex plane. In 2-D space, the rotation axis is unique, except for the *direction* of rotation. Therefore, the polar representation of a complex number $z = x + iy$ is uniquely defined by $(r, \varphi) = (\sqrt{z\bar{z}}, \arg(z))$, where $\arg(z)$ is given by

$$\arg(z) = \text{atan2}(y, x) = \text{sign}(y)\text{atan}(|y|/x)$$

with $\text{atan}(\cdot) \in [0, \pi)$. The factor $\text{sign}(y)$ indicates the direction of rotation. If we use this definition, the negative real numbers are singular because they have an angle of π with respect to positive *and* negative rotations.

In 3-D space, the rotation axis is represented by a 3-D unit vector. The straightforward generalization of a 2-D angle is then a vector with the length corresponding to the rotation angle and the direction corresponding to the rotation axis. This vector is called the *rotation vector*. Consequently, we define a new arctangent function by the rotation vector that represents the rotation of $(0,0,|\mathbf{x}|)^\top$ into $\mathbf{x}$ (with $\mathbf{x} \neq 0$; see also Fig. 6):

$$\text{atan3}(\mathbf{x}) = \frac{\mathbf{x}_D}{|\mathbf{x}_D|}\text{atan}\left(\frac{|\mathbf{x}_D|}{\langle(0,0,1)^\top,\mathbf{x}\rangle}\right) \tag{14}$$

where $\mathbf{x}_D = (0,0,1)^\top \times \mathbf{x}$ yields the direction of the rotation vector. Again, there is a singularity if $\mathbf{x} = (0,0,-|\mathbf{x}|)^\top$, but now, it becomes more obvious why this is a singularity: The magnitude of the rotation vector is well defined by π, but the rotation axis is arbitrary in the 2-D subspace orthogonal to $\mathbf{x}$. Therefore, *any* rotation vector in that subspace is a solution of (14).

If we have a smooth vector field and we want to use (14) as a definition of the *phase* of the vector field (as we will do in the next paragraph), it is possible to extend the definition: If we consider the values of (14) in an open sphere with radius ε around the singular point and let ε tend to zero while averaging the rotation directions, we get a well-defined rotation vector because of the smoothness of the vector field. This continuous extension of the orientation is used in [25] for a stable orientation estimation.

Using (14), we are able to define the phase of the monogenic signal (abbreviation: monogenic phase) by

$$\varphi(\mathbf{x}) = \text{atan3}(\mathbf{f}_M(\mathbf{x})) \stackrel{\text{def}}{=} \arg(f_M(\mathbf{x})) \tag{15}$$

where $\mathbf{f}_M$ is the vector field such that $f_M = (i,j,1)\mathbf{f}_M$. The rotation vector field $\varphi(\mathbf{x}) = (\varphi_1(\mathbf{x}),\varphi_2(\mathbf{x}),\varphi_3(\mathbf{x}))^\top$ represents the rotation of the real-valued signal $|f_M(\mathbf{x})|$ into the quaternionic-valued signal $f_M(\mathbf{x})$. Note that the real component is the third component of the 3-D vector.

The rotation vector φ always lies in the plane orthogonal to $(0,0,1)^\top$ since $\mathbf{x}_D = (-x_2,x_1,0)^\top$, and hence, $\varphi_3 = 0$. Comparable with phase wrapping in 1-D, there is a *wrapping of the phase vectors* of the monogenic phase: If a vector in a certain direction would exceed the amplitude π, it is replaced by the vector minus 2π times the unit vector in that direction, i.e., it points in the opposite direction; see Fig. 4.

In Section IV-B, we already used the norm of the quaternions for calculating the energy of a monogenic signal. Indeed, the norm is used for defining the *local amplitude* of $f_M(\mathbf{x})$ by

$$\begin{aligned}|f_M(\mathbf{x})| &= \sqrt{f_M(\mathbf{x})\bar{f}_M(\mathbf{x})} \\ &= \sqrt{f^2(\mathbf{x}) + |\mathbf{f}_R(\mathbf{x})|^2}.\end{aligned} \tag{16}$$

The choice of definitions for the local phase (15) and local amplitude (16) establishes a *transformation to polar coordinates*. Given the local phase $\varphi(\mathbf{x})$ and the local amplitude $|f_M(\mathbf{x})|$ of a monogenic signal, it can be reconstructed by

$$f_M(\mathbf{x}) = |f_M(\mathbf{x})|\exp((-j,i,0)\varphi(\mathbf{x})). \tag{17}$$

Fig. 4. Monogenic phase of one part of Fig. 3, left (curved line, displayed as underlying grayscale image). The phase is represented by the vector field that is obtained according to (15). Hence, the length indicates the rotation angle, and the direction indicates the rotation axis. Note the phase wrapping.

To see this, observe that from $(-j,i,1)\varphi = i\varphi_2 - j\varphi_1$, we get

$$\exp(i\varphi_2 - j\varphi_1) = \cos|\varphi| + i\frac{\varphi_2}{|\varphi|}\sin|\varphi| - j\frac{\varphi_1}{|\varphi|}\sin|\varphi|$$

and

$$\mathbf{x}_D = \frac{\sin|\varphi|}{|\varphi|}(\varphi_1,\varphi_2,0)^\top.$$

Plugging (14) into (15) yields

$$\arg(\exp(i\varphi_2 - j\varphi_1)) = \frac{(\varphi_1,\varphi_2,0)^\top}{|\varphi|}\text{atan}\left(\frac{\sin|\varphi|}{\cos|\varphi|}\right) = \varphi.$$

In the previous section, the property "split of identity" was discussed only with respect to the isotropy of the energy (or amplitude). Now, having a definition of the monogenic phase, we recognize that amplitude and phase are indeed orthogonal. The local amplitude includes energetic information, and the phase includes structural information. In contrast to the 1-D case, the phase now includes additional *geometric information*. The orthogonality of structural and geometric information is discussed at the end of the next section.

B. Relation to the 1-D Analytic Signal

Up until now, we have considered the 1-D analytic signal and the 2-D monogenic signal as two approaches that are only related by the fact that the latter is the generalization of the former with respect to the dimension of the domain. In signal theory, there is a well-known relation between 1-D and 2-D signals: the Radon transform [26]. The Radon transform $\mathcal{R}$ maps a 2-D signal onto an orientation parameterized family of 1-D signals by integrating the 2-D signal on the line given by the orientation parameter:

$$\mathcal{R}\{f\}(t,\theta) = \int_{\mathbb{R}^2} f(\mathbf{x})\delta_0(\langle\mathbf{x},\mathbf{n}_\theta\rangle - t)\,d\mathbf{x} \tag{18}$$

where $\delta_0(\cdot)$ is the Dirac delta, and $\mathbf{n}_\theta = (\cos\theta,\sin\theta)^\top$ is the normal vector given by the orientation[5] $\theta \in [0,\pi)$. Geometrically, the Radon transform projects (orthogonally) the 2-D

[5]Note the difference between *direction* and *orientation* in this context: a direction corresponds to a vector, an orientation to a 1-D subspace.

signal onto a line with orientation θ. The Radon transform is invertible, and there are some important theorems about signals in the Radon domain, such as the Fourier slice theorem [4]:

$$\mathcal{F}_1\{\mathcal{R}\{f\}\}(u,\theta) = F(u\mathbf{n}_\theta). \tag{19}$$

As a consequence of the slice theorem, the Radon transform relates the Riesz transform of a 2-D signal to the Hilbert transforms of the 1-D signals obtained from the Radon transform.[6] Accordingly, we conclude that the interpretation of the monogenic phase of intrinsically 1-D signals in 2-D space is the same as the interpretation of the complex phase in 1-D space. However, for intrinsically 2-D signals, we also obtain an interpretation by decomposing the signal into its intrinsically 1-D parts. Indeed, the Radon transform is the connecting link between the 1-D and 2-D approaches.

The Radon transform of the $\mathbb{H}$-embedded Riesz transform $f_R(\mathbf{x}) = (i,j)\mathbf{f}_R(\mathbf{x})$ [embedded in $\mathbb{H}$ according to (12)] of a 2-D signal $f(\mathbf{x})$ is given by the Hilbert transform of the Radon transform of $f(\mathbf{x})$ according to

$$\mathcal{R}\{f_R\}(t,\theta) = (i,j)\mathbf{n}_\theta\, h_1(t) * \mathcal{R}\{f\}(t,\theta). \tag{20}$$

This equivalence can easily be shown in the Fourier domain, using the linearity of the Radon, Riesz, Hilbert, and Fourier transforms:

$$\begin{aligned}\mathcal{F}_1\{\mathcal{R}\{f_R\}\}(u,\theta) &\overset{(19)}{=} (i,j)\mathbf{F}_R(u\mathbf{n}_\theta)\\ &= (i,j)i\frac{u\mathbf{n}_\theta}{|u\mathbf{n}_\theta|}F(u\mathbf{n}_\theta)\\ &= (i,j)\mathbf{n}_\theta\, H_1(u)\mathcal{F}_1\{\mathcal{R}\{f\}\}(u,\theta).\end{aligned}$$

Hence, the Radon transform allows us to calculate the Riesz transform (and, therefore, the monogenic signal as well) by using the Hilbert transform (see also Fig. 5).

This can be used to circumvent application of the Riesz transform in the Fourier domain [actually, application in the spatial domain is not very reasonable due to the infinite extent of the impulse response; see (11)]. Especially in applications where the data is given in the Radon domain (e.g., X-ray tomography), it is advantageous to have this equivalence. By the following algorithm, we get the monogenic signal directly from data given in the Radon domain.

1) Calculate the Hilbert transform $\mathcal{R}\{f\}_H = h_1 * \mathcal{R}\{f\}$.
2) Multiply $\mathcal{R}\{f\}_H$ by $\cos\theta$ and $\sin\theta$.
3) Calculate the inverse Radon transform of $\mathcal{R}\{f\}$, $\cos\theta\,\mathcal{R}\{f\}_H$, and $\sin\theta\,\mathcal{R}\{f\}_H$.

Having the monogenic signal, we can apply other algorithms for estimating local properties, detecting features, etc. (see [25]).

A second application of (20) is the design of *spherical quadrature filters* (SQFs) with finite spatial extent. As with a 1-D quadrature filter (QF), which is a Hilbert pair of bandpass filters, an SQF is a Riesz triple of bandpass filters. Filters with finite extent can only be obtained by an optimization, as in the 1-D case. The following algorithm produces optimized filters using optimized 1-D QFs and an optimized inverse Radon transform (see e.g., [4]).

[6]Actually, this relationship, as well as the Riesz transform, are well covered by the results from Calderón–Zygmund theory [27], which is not very accessible to engineers and computer scientists due to its abstract mathematical formulation. Therefore, we think that calculus-based derivations of these results are helpful.

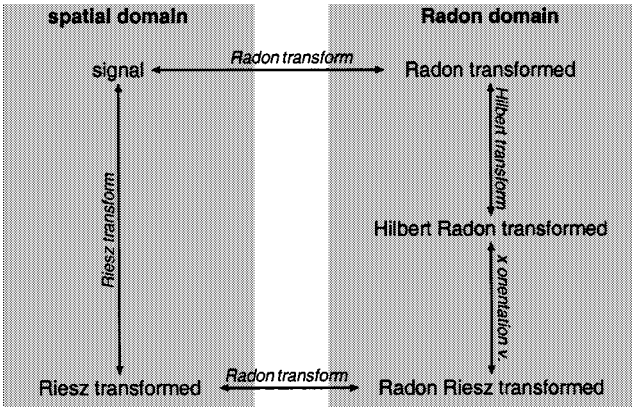

Fig. 5. Relation between Radon, Riesz, and Hilbert transform. The Riesz transform in the spatial domain (left) is equivalent to the Hilbert transform with subsequent multiplication by the orientation vector in the Radon domain (right).

1) Choose an optimized 1-D QF with appropriate size (this size will later be the radius of the SQF).
2) Create the Radon Riesz transformed signal by multiplying the odd part of the 1-D QF with $\cos\theta$ and $\sin\theta$.
3) Apply the (optimized) inverse Radon transform.

The triple of filters obtained by this procedure can be applied to a 2-D signal (image) by convolutions, resulting in the bandpass filtered monogenic signal of the image.

A third consequence of (20) is that the interpretation of the monogenic phase is given directly by the phase of the analytic signal since

$$\begin{aligned}\mathcal{R}\{f_M\}(t,\theta) &= \mathcal{R}\{f\}(t,\theta) - \mathcal{R}\{f_R\}(t,\theta)i\\ &= \mathcal{R}\{f\}(t,\theta) - (i,j)\mathbf{n}_\theta h_1(t) * \mathcal{R}\{f\}(t,\theta)\\ &= (i,j,1)\mathbf{R}(\theta)(-h_1 * \mathcal{R}\{f\}, 0, \mathcal{R}\{f\})^\top\end{aligned}$$

where $\mathbf{R}(\theta)$ is the rotation about the real axis by θ. Evaluating the last line for $\theta = 0$ gives

$$\mathcal{R}\{f\}(t,\theta) - ih_1(t) * \mathcal{R}\{f\}(t,\theta)$$

i.e., the analytic signal of $\mathcal{R}\{f\}(t,\theta)$. For any $\theta = \theta_0$, the Radon transform of the monogenic signal is just the analytic signal of the Radon transform of the signal but with the imaginary unit i rotated by θ_0: $\exp(k\theta_0)i = \cos\theta_0 i + \sin\theta_0 j$. The impact of this result on the interpretation of the monogenic phase is that for linear structures with large support (lines, edges in images), the Radon transform is dominated by this structure. Hence, the monogenic phase is given by the main orientation θ_0 and the 1-D phase of $\mathcal{R}\{f\}(t,\theta_0)$. In the idealized case (i.e., the signal is constant in one direction), the Radon transform is nonzero only for the main orientation. Accordingly, the $(i,j)\mathbf{n}_\theta$ in (20) is constant (equals $(i,j)\mathbf{n}_{\theta_0}$), and the Riesz transform is given by

$$f_R(\mathbf{x}) = (i,j)\mathbf{n}_{\theta_0}(\delta_0(\langle \mathbf{x}, \mathbf{n}_{\theta_0}^\perp\rangle)h_1(\langle \mathbf{x}, \mathbf{n}_{\theta_0}\rangle)) * f(\mathbf{x}).$$

Thus, (20) is simplified to Theorem 1 in [28]. In contrast to the idealized case, (20) also provides a sensible interpretation for nonperfect signals.

For an intrinsically 1-D signal, we get the following decomposition of the phase vector (15) while keeping the local phase of the underlying 1-D signal. The rotation vector $\varphi(\mathbf{x})$ is orthogonal to the *local orientation* (i.e., the orientation of the Dirac line

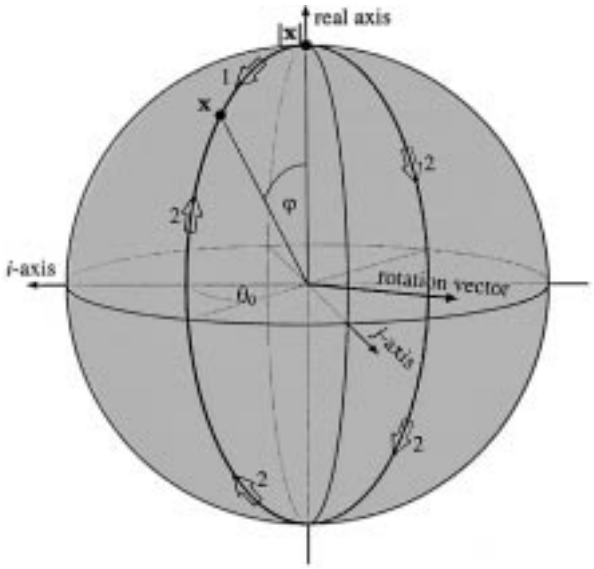

Fig. 6. Phase representation using a rotation vector φ. First, the real value $|\mathbf{x}|$ is rotated about the second axis (j-axis) by φ and second about the third axis (real axis) by θ_0. The rotation vector is orthogonal to the plane spanned by the real axis and the vector $\mathbf{x}$. Its length is given by the angle between the real axis and $\mathbf{x}$. Although the rotation vector is unique, the decomposition is not. There are two possibilities: 1) (θ_0, φ) and 2) $(\theta_0 + \pi, -\varphi)$.

in the Fourier domain) of the 2-D signal, and $-\text{sign}(\varphi_1)|\varphi(\mathbf{x})|$ represents the *local 1-D phase* of the 2-D signal (see also Fig. 6). These interpretations are consistent with the former definition of local phase and local orientation in [13].

Note that these definitions do not yield a unique phase representation since a rotation of the signal by π yields the same orientation and a negated phase. This ambiguity can be visualized by two different decompositions of the rotation vector (see Fig. 6). The same problem also occurs in the context of oriented quadrature filters (see [5]), where Granlund and Knutsson claim that there is no local way to get the direction from the orientation. In [29] and [30], it is proposed to apply an unwrapping of the orientation (modulo 2π) in order to obtain a consistent phase representation. The application in both papers is the 2-D demodulation needed for interferogram processing.

If the monogenic phase is decomposed into local orientation and local phase, the split of identity (the third property of the analytic signal) is also preserved with respect to geometric and structural information. The local phase is invariant to changes of the local orientation, and the local orientation is invariant to changes of the local structure (up to the ambiguity explained above). If we can recover the correct local direction from the local orientation, we have an ideal split of identity with respect to energetic, geometric, and structural information. The problem with the correct local direction is that there is no absolute solution; there is only a relative one. This relative solution can be obtained by constraints on the smoothness of the phase and orientation.

VI. Conclusion

In the present paper, we have analytically derived the monogenic signal, which is a generalization of the analytic signal to two dimensions. This new 2-D analytic signal is based on the Riesz transform and preserves the properties of the 1-D analytic signal. In contrast to previous approaches, it is isotropic and, therefore, performs a split of identity. The information included in the signal is orthogonally decomposed into energetic, structural, and geometric information by means of local amplitude, local phase, and local orientation. We have established an equality that directly relates the 1-D analytic signal and the 2-D monogenic signal. The Radon transform was shown to be the appropriate tool for shifting the 1-D Hilbert transform to 2-D.

One can imagine a wide field of possible applications of the monogenic signal. Up to now, several applications have been realized, for example

- estimation of the local orientation;
- contrast independent edge detection (see both in [25]);
- Moiré interferograms [29], [30];
- texture analysis [28];
- image denoising [31];
- curvature estimation and corner detection [14];
- stereo correspondence.

Both the monogenic signal and its applications are easier to formulate in geometric algebra. It is even possible to generalize the approach to arbitrary dimensions [18]. Nevertheless, we chose the vector notation since it is more common. It was only necessary to formulate some details using quaternions (which is a specific geometric algebra) in order to have the tools for geometric computations available. For applications, however, it is not necessary to make use of geometric algebra. The monogenic signal is obtained by ordinary real-valued convolution kernels.

Appendix

The algebra of quaternions is not widely known in the signal processing community. Therefore, we give a short introduction in this Appendix. In Section II, we defined the quaternions to be the algebra on the real 4-D vector space spanned by $\{1, i, j, k\}$ (i.e., a quaternion is of the form $q = q_1 + q_2 i + q_3 j + q_4 k$) with the algebra product defined by $i^2 = j^2 = -1$ and $ij = -ji = k$. From these two rules, we can derive all other products of base elements since $k^2 = -ijji = -1, ik = -j = -ki$, and $jk = i = -kj$. Addition and subtraction of quaternions is given by vector addition $(p = p_1 + p_2 i + p_3 j + p_4 k)$

$$q + p = (q_1 + p_1) + (q_2 + p_2)i + (q_3 + p_3)j + (q_4 + p_4)k$$

and multiplication with a real number λ by field multiplication

$$\lambda q = (\lambda q_1) + (\lambda q_2)i + (\lambda q_3)j + (\lambda q_4)k.$$

The multiplication of two arbitrary quaternions is obtained by associativity and distributivity

$$\begin{aligned} qp = {} & (q_1 p_1 - q_2 p_2 - q_3 p_3 - q_4 p_4) \\ & + (q_1 p_2 + q_2 p_1 + q_3 p_4 - q_4 p_3)i \\ & + (q_1 p_3 + q_3 p_1 - q_2 p_4 + q_4 p_2)j \\ & + (q_1 p_4 + q_4 p_1 + q_2 p_3 - q_3 p_2)k. \end{aligned}$$

The conjugate of a quaternion q is defined by

$$\bar{q} = q_1 - q_2 i - q_3 j - q_4 k$$

so that the norm of q is

$$|q| = \sqrt{q\bar{q}} = \sqrt{q_1^2 + q_2^2 + q_3^2 + q_4^2}.$$

Additionally, the quaternions are a division algebra, which means that the inverse of a quaternion is uniquely given by $q^{-1} = (\bar{q}/|q|^2)$. The exponential function of a quaternion q is defined by

$$\exp(q) = \sum_{n=0}^{\infty} \frac{q^n}{n!}$$

(which converges since $\exp(|q|)$ converges), and any linear combination of i and j with unit magnitude can be substituted for the imaginary unit in the Euler formula

$$\exp(ai + bj) = \cos\sqrt{a^2+b^2} + \frac{ai+bj}{\sqrt{a^2+b^2}} \sin\sqrt{a^2+b^2}.$$

Hence, the only fundamental difference to working with complex numbers is that the base elements i, j, k do not commute. For a more detailed introduction of quaternions, see, e.g., [32].

ACKNOWLEDGMENT

The authors would like to thank N. Krüger for many fruitful discussions.

REFERENCES

[1] B. Milkereit and C. Spencer, "Multiattribute processing of seismic data: Application to dip displays," *Can. J. Explor. Geophys.*, vol. 26, no. 1 & 2, pp. 47–53, Dec. 1990.
[2] A. I. Zayed, *Handbook of Function and Generalized Function Transformations*. Boca Raton, FL: CRC, 1996.
[3] W. Osten, *Digitale Verarbeitung und Auswertung von Interferenzbildern*. Berlin, Germany: Akademie Verlag, 1991.
[4] B. Jähne, *Digitale Bildverarbeitung*. Berlin, Germany: Springer-Verlag, 1997.
[5] G. H. Granlund and H. Knutsson, *Signal Processing for Computer Vision*. Dordrecht, The Netherlands: Kluwer, 1995.
[6] P. Kovesi, "Invariant Measures of Image Features from Phase Information," Ph.D. dissertation, Univ. Western Australia, Perth, 1996.
[7] M. Hansen, "Stereosehen—ein verhaltensbasierter Ansatz," Ph.D. dissertation, Christian Albrechts Univ., Kiel, Germany, 1998.
[8] A. V. Oppenheim and J. S. Lim, "The importance of phase in signals," *Proc. IEEE*, vol. 69, pp. 529–541, May 1981.
[9] N. K. Bose, "Trends in multidimensional systems theory," in *Multidimensional Systems Theory*, N. K. Bose, Ed. Dordrecht, The Netherlands: D. Reidel, 1985, pp. 1–40.
[10] M. Nieto-Vesperinas, "Dispersion relations in two dimensions: Application to the phase problem," *Optik*, vol. 56, no. 4, pp. 377–384, 1980.
[11] T. Bülow, "Hypercomplex Spectral Signal Representations for the Processing and Analysis of Images," Ph.D. dissertation, Christian Albrechts Univ., Kiel, Germany, 1999.
[12] G. Krieger and C. Zetzsche, "Nonlinear image operators for the evaluation of local intrinsic dimensionality," *IEEE Trans. Image Processing*, vol. 5, pp. 1026–1041, June 1996.
[13] M. Felsberg and G. Sommer. (2000, Feb.) Structure multivector for local analysis of images. Institute of Computer Science and Applied Mathematics, Christian Albrechts Univ., Kiel, Germany. [Online]. Available: http://www.ks.informatik.uni-kiel.de.
[14] ——, "The structure multivector," in Applied Geometrical Algebras in Computer Science and Engineering. Boston, MA: Birkhäuser, 2001, to be published.
[15] D. Hestenes and G. Sobczyk, *Clifford Algebra to Geometric Calculus, A Unified Language for Mathematics and Physics*. Dordrecht, The Netherlands: Reidel, 1984.
[16] G. Sommer, Ed., *Geometric Computing with Clifford Algebras*. Heidelberg, Germany: Springer-Verlag, 2001.
[17] F. Brackx, R. Delanghe, and F. Sommen, *Clifford Analysis*. Boston, MA: Pitman, 1982.
[18] M. Felsberg and G. Sommer, "The multidimensional isotropic generalization of quadrature filters in geometric algebra," in *Proc. Int. Workshop Algebraic Frames Perception-Action Cycle*, vol. 1888, G. Sommer and Y. Y. Zeevi, Eds, Heidelberg, Germany, Sept. 2000, pp. 175–185. *Lecture Notes in Computer Science*.
[19] S. L. Hahn, *Hilbert Transforms in Signal Processing*. Boston, MA: Artech House, 1996.
[20] T. A. Ell, "Hypercomplex spectral transformations," Ph.D. dissertation, Univ. Minnesota, Minneapolis, 1992.
[21] S. G. Krantz, *Handbook of Complex Variables*. Boston, MA: Birkhäuser, 1999.
[22] E. M. Stein and G. Weiss, *Introduction to Fourier Analysis on Euclidean Spaces*. Princeton, NJ: Princeton Univ. Press, 1971.
[23] M. N. Nabighian, "Toward a three-dimensional automatic interpretation of potential field data via generalized Hilbert transforms: Fundamental relations," *Geophys.*, vol. 49, no. 6, pp. 780–786, June 1984.
[24] R. N. Bracewell, *Two-Dimensional Imaging*. Englewood Cliffs, NJ: Prentice-Hall, 1995.
[25] M. Felsberg and G. Sommer, "A new extension of linear signal processing for estimating local properties and detecting features," in *Proc. 22nd DAGM Symp. Mustererkennung*, G. Sommer, N. Krüger, and C. Perwass, Eds., Heidelberg, Germany, 2000, pp. 195–202.
[26] J. Radon, "On the determination of functions from their integral values along certain manifolds," *IEEE Trans. Medical Imaging*, vol. MI–5, pp. 170–176, Dec. 1986.
[27] E. M. Stein, "Singular integrals: The roles of Calderón and Zygmund," in *Notices Amer. Math. Soc.*, vol. 45, 1998, pp. 1130–1140.
[28] M. Felsberg and G. Sommer, "Structure multivector for local analysis of images," in *Multi-Image Analysis*, R. Klette, T. Huang, and G. Gimel'farb, Eds. Berlin, Germany: Springer-Verlag, 2001, vol. 2032, pp. 95–106. *Lecture Notes in Computer Science*.
[29] T. Bülow, D. Pallek, and G. Sommer, "Riesz transforms for the isotropic estimation of the local phase of moire interferograms," in *22nd DAGM Symp. Mustererkennung*, G. Sommer, Ed., Heidelberg, Germany, 2000.
[30] K. G. Larkin, D. J. Bone, and M. A. Oldfield, "Natural demodulation of two-dimensional fringe patterns: I. General background of the spiral phase quadrature transform," *J. Opt. Soc. Amer. A*, vol. 18, no. 8, pp. 1862–1870, 2001.
[31] M. Felsberg and G. Sommer, "Scale adaptive filtering derived from the Laplace equation," presented at the 23rd DAGM Symp. Mustererkennung, vol. 2191, B. Radig and S. Florczyk, Eds., Heidelberg, Germany, 2001. *Lecture Notes in Computer Science*.
[32] P. Lounesto, *Clifford Algebras and Spinors*: Cambridge Univ. Press, 1997, vol. 239. London Math. Soc. Lecture Note Series.

Michael Felsberg was born in Preetz, Germany, in 1974. He received the diploma degree in engineering from Christian Albrechts University Kiel, Kiel, Germany, in 1998, where he is pursuing the Ph.D. degree.

He is currently with the Cognitive Systems Group, Kiel University. His research interests include multidimensional signal theory, image processing, and low-level computer vision by means of geometric algebra and Clifford analysis. He holds a scholarship for his Ph.D. studies from the German National Merit Foundation (Studienstiftung des Deutschen Volkes).

Mr. Felsberg is a member of the DFG Graduiertenkolleg no. 357.

Gerald Sommer received the diploma and the Ph.D. degrees from Friedrich Schiller University, Jena, Germany, both in physics, in 1969 and 1975, respectively, and the habilitation degree in engineering from Technical University Ilmenau, Ilmenau, Germany, in 1988.

From 1969 to 1991, he worked with several departments of the Friedrich Schiller University. From 1991 to 1993, he was the head of the division for medical image processing at the Research Center for Environment and Health (GSF-Medis), Munich-Neuherberg. Since 1993, he has been Professor of computer science with the Christian Albrechts University Kiel, Kiel, Germany. He leads the cognitive systems research group. Currently, his main interestis the design of behavior-based systems. His research covers signal theory and signal processing, neural computation for pattern recognition, computer vision, and robot control.